

## Adaptive tunicate swarm optimization with partial transmit sequence for phase optimization in MIMO-OFDM

Abdul Lateef Haroon Phulara Shaik<sup>1</sup>, Sowmya Madhavan<sup>2</sup>, Parameshchhari Bidare Divakarachari<sup>2</sup>,  
Rocío Pérez de Prado<sup>3</sup>, Paramesh Siddappa Parameshwarappa<sup>4</sup>,  
Kavitha Malali Vishveshwarappa Gowda<sup>5</sup>

<sup>1</sup>Department of Electronics and Communication Engineering, Ballari Institute of Technology and Management, Ballari, India

<sup>2</sup>Department of Electronics and Communication Engineering, Nitte Meenakshi Institute of Technology, Bengaluru, India

<sup>3</sup>Department of Telecommunication Engineering, University of Jaén, Linares, Spain

<sup>4</sup>Department of Computer Science and Engineering, School of Engineering, Central University of Karnataka, Kalaburagi, India

<sup>5</sup>Department of Electronics and Communication Engineering, Gopalan College of Engineering and Management, Bangalore, India

### Article Info

#### Article history:

Received Dec 23, 2023

Revised Feb 2, 2024

Accepted Mar 21, 2024

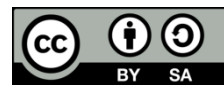
#### Keywords:

Adaptive tunicate swarm optimization  
Fast Fourier transform  
Multiple-input multiple-output  
Nonsquare-matrix-based differential space time coding  
Orthogonal frequency division multiplexing  
Peak-to-average-power ratio

### ABSTRACT

Multiple-input multiple-output (MIMO) and orthogonal frequency division multiplexing (OFDM) are widely utilized in wireless systems and maximum data rate communications. The MIMO-OFDM technology increases the efficiency of spectrum utilization. The peak-to-average-power ratio (PAPR) minimization in MIMO-OFDM is a complex task in wireless communications systems. In this research, an adaptive tunicate swarm optimization with partial transmit sequence (ATSO-PTS) algorithm is proposed for a reduction of PAPR in MIMO-OFDM. The nonsquare-matrix-based differential space time coding (N-DSTC) scheme is used for the encoding and decoding process of MIMO-OFDM. The N-DSTC encoding and decoding are linear error-correcting codes that are utilized for message transmission over noisy channels. The pre-specified quadrature phase shift keying (QPSK) symbol is deployed for the modulation and demodulation scheme. On the receiver side, the serial to parallel (S/P) conversion, and fast Fourier transform (FFT) are accomplished, alongside the received data bits being demodulated to obtain the output bits. The proposed ATSO-PTS method achieves better results according to performance metrics PAPR, bit error rate (BER) and signal-to-noise-ratio (SNR), with values of about 2.9, 0.01 and 0.025, respectively. This ensures superior results when compared to the existing methods of twin symbol hybrid optimization applied to partial transmit sequence (TSHO-PTS), selective level mapping and PTS (SLM-PTS), and particle swarm and grey wolf (PS-GW) with PTS, respectively.

This is an open access article under the [CC BY-SA](https://creativecommons.org/licenses/by-sa/4.0/) license.



### Corresponding Author:

Parameshchhari Bidare Divakarachari

Department of Electronics and Communication Engineering, Nitte Meenakshi Institute of Technology

P.B.No.6429, Yelahanka, Bangalore 560064, Karnataka, India

Email: paramesh@nmit.ac.in

## 1. INTRODUCTION

The growing need for advancements in wireless applications has rendered the currently available radio frequency (RF) spectrum, inadequate to meet future service requirements [1]. Orthogonal frequency division multiplexing (OFDM) is majorly considered in wireless systems to attain maximum-rate data transmission due to its larger spectral efficiency, simple equalization, as well as low-complexity execution [2], [3]. Therefore, OFDM is also majorly utilized in wideband communications over mobile radio channels, digital audio broadcasting, high-bit-rate digital subscriber lines and optical systems [4]. Despite the OFDM

having number of advantages, it has one major limitation, which is that the transmitted signal has a high peak-to-average-power ratio (PAPR) [5]. On an assumption of maximum PAPR, the OFDM signal is fasten when it forwards by non-linear high-power amplifier (HPA) and thus, the performance is degenerated, while in-band bias as well as out-of-band radiation also happens. Thus, the OFDM transmitters needs costly linear HPA with extreme dynamic range [6], [7]. Recently, a number of optimization algorithms are recommended to optimize the partial transmit sequence (PTS) technique for PAPR reduction in OFDM systems [8]. Between them, the most famous evolutionary algorithms are the genetic algorithm (GA), differential evolutionary algorithm (DE), and biogeographic optimization algorithm (BBO) which are majorly used for the reduction of PAPR [9]. However, the selection of the phase factor sequence in the PTS approach is a risk in non-linear optimization, which is caused by greater complexity and memory utilization if there are a greater number of non-overlapping sub-blocks [10], [11]. By embedding the pilot signal within the optical OFDM signal in the frequency domain minimizes the time domain signals [12]. A reduction of PAPR in MIMO-OFDM is a complex task in wireless communications, where the spectral efficiency is also reduced when the cyclic prefix enters in OFDM [13]. According to the literature and targetted at the limitations of an existing signal compounding transform methods, a novel approach is introduced for combinely optimize the PAPR and bit error rate (BER) performance [14], [15].

Sarkar *et al.* [16] implemented a twin symbol hybrid optimization applied to partial transmit sequence (TSHO-PTS) to minimize PAPR in cyclic prefix-OFDM (CP-OFDM). The hybrid optimization algorithms of salp swarm (SS) as well as bald eagle search (BES) were produced to determine phase factor. The digital chaotic was utilized to certify physical layer security in data transmission for (DFT-S-OFDM) subcarrier allocation. A PTS method achieved the minimum PAPR in less processed and consumed time, but the efficiency of bandwidth was decreased by the system itself. Sidiq *et al.* [17] developed a hybrid method of selective level mapping and PTS (SLM-PTS) with ant bee colony (ABC) phase optimization for PAPR minimization. The SLM was initially enforced to the traditional farnesyl dimethyl chromanol (FDMC) signal and the PAPR signal was obtained with selected similar phase sequences. This method significantly minimized the PAPR by the minimum computational complexity by combining the SLM and PTS benefits. The SLM-PTS suffered from the interface between unsynchronized symbols in the closest bands. Kumar *et al.* [18] implemented a PTS over a hybrid of particle swarm and grey wolf (PS-GW) optimization for the performance of minimum PAPR, as well as low computational complexity. The PS-GW identified the phase rotational factors combination effectively. The PS exploitation was improved with the estimation capability in GW to develop multiple variations in quality. The PS-GW achieved better performance and minimum PAPR than the PS and GW. However, PAPR achievement was decreased using various channel constraints. Prasad and Jayabalan [19] implemented a particle swarm optimization (PSO) applied to the technique of PTS to identify the phase factor for reducing the PAPR. A scaling factor was established in the velocity updating equation of conventional PSO to enhance the inertia weight and particle velocity. The PSO-PTS achieved the efficient minimum PAPR and was most efficient for the applications using the 64-quadratic amplitude modulation (QAM) modulation scheme, but this method performed a low convergence rate.

Şimsir and Taşpınar [20] implemented a discrete elephant herding optimization using PTS (DEHO-PTS) to minimize PAPR in universal-filtered multi-carrier (UFMC) signals to the lowest levels. An advanced scheme of PTS was powered by an intelligent optimization which was enforced to UFMC waveform. This approach was majorly focused on decreasing the transmission signals in PAPR values and achieved better performance and low BER. The conventional PTS was a difficult method for systems to obtain efficient transmission powers with a smaller number of searches. Bai and Yang [21] developed an enhanced PSO called the discrete adaptive PSO (DAPSO) approach for solving the problem of high PAPR in UOWC. This method integrated PTS and DAPSO to minimize the PAPR in the UOWC system. The PTS was applied to a probabilistic approach for effectively defeating the performance of PAPR. Simultaneously, the two-dimensional adaptive PSO effectively modified the comprehensive search for the phases of PTS. This method effectively solved the complexity of the calculation and also achieved a fast convergence speed. Abed *et al.* [22] introduced PSO-based dummy sub-carriers which were applied with data, without transmitting the side information for PAPR reduction. The fusion of suggested approach was employed by calculating a PAPR at an outcome of inverse fast fourier transform (IFFT). Later, this method added the six adaptive sub-carrier sequences to an IFFT input data. This method transmitted the data when the dummy sub-carrier was in a significant threshold. Further, it utilized the additive white gaussian noise (AWGN) channel to explore the performance of PAPR and BER. This method achieved low computational complexity regarding the number of additions and multiplications, but it had a low convergence rate. Li *et al.* [23] developed a PTS-based discrete PSO with a threshold (PTS-DPSO-TH) and utilized to a filter bank multi-carrier with quadratic amplitude modulation (FBMC/OQAM) for PAPR reduction. This method utilized the DPSO to identify an optimal solution and effectively minimize the PAPR in the OQAM approach, alongside reducing the complexity problem. Then, the threshold was established to minimize the iteration numbers, and

later decrease the system complication on the assumption of undertaking the PAPR reduction performance. The PTS-DPSO-TH effectively reduced the PAPR, but this approach had a low convergence rate.

Şimsir and Taşpınar [24] introduced an efficient PAPR reduction method for the waveform of the UFMC system. This method initially introduced a novel discrete version of the invasive weed optimization (DIWO) approach and combined it with the traditional PAPR reduction approach called PTS deployed as the phase optimizer. By doing so, this method acquired a novel method known as DIWO-PTS. The DIWO was the method to optimize the phase sequences in the discrete phase. The DIWO achieved the best phase integration in a minimum number of searches. However, the DIWO had less population diversity and did not take the best member of the population during the process of optimization. Ali and Hamza [25] implemented a new optimization method, teaching-learning-based optimization (TLBO) for the reduction of PAPR in the OFDM signal. This approach introduced selective mapping (SLM) based TLBO for the effective reduction. The TLBO was performed to identify search factors in the SLM approach. This method effectively reduced the PAPR with low computational complexity and did not require certain parameters. However, this method consumed a larger memory storage space. To address these limitations of the existing methods, the MIMO-OFDM systems are proposed in this research. Simultaneously, the synchronization, evaluation of channel, PAPR, larger memory storage, selection of antenna, and convergence rate were the specific limitations of the above-discussed existing methods which are examined through the OFDM signal. Therefore, for the reduction of PAPR, the novel adaptive tunicate swarm optimization with partial transmit sequence (ATSO-PTS) with MIMO-OFDM approach is introduced to minimize PAPR in OFDM. Further, the proposed method is briefly discussed in the following section. This research's major contributions are as follows:

- This research offers the reduction of PAPR with faster convergence as well as minimized computational complexity as the foremost achievement.
- The paper focuses on minimizing PAPR using quick convergence and minimizing computational complexity. The ATSO-PTS is developed for PAPR reduction in MIMO-OFDM.
- Nonsquare-matrix-based differential space time coding (N-DSTC) approach is employed for encoding and decoding which helps to achieve better data broadcasting over the MIMO-OFDM. This research considers quadrature phase shift keying (QPSK) for modulation/demodulation because of its low error probability.

The rest of the paper is arranged in the succeeding way: section 2 presents the proposed methodology which includes the MIMO-OFDM system with N-DSTC encoding and decoding approaches. Section 3 discusses the ATSO. Section 4 describes results and discussion and finally, section 5 describes the overall summary.

## 2. PROPOSED METHOD

In this research, an ATSO is proposed with the N-DSTC coding for minimizing PAPR while transmitting the data over MIMO-OFDM. The N-DSTC codes are linear error-correcting codes that are utilized for the transmission of messages over noisy channels. Figure 1 depicts the proposed method's workflow.

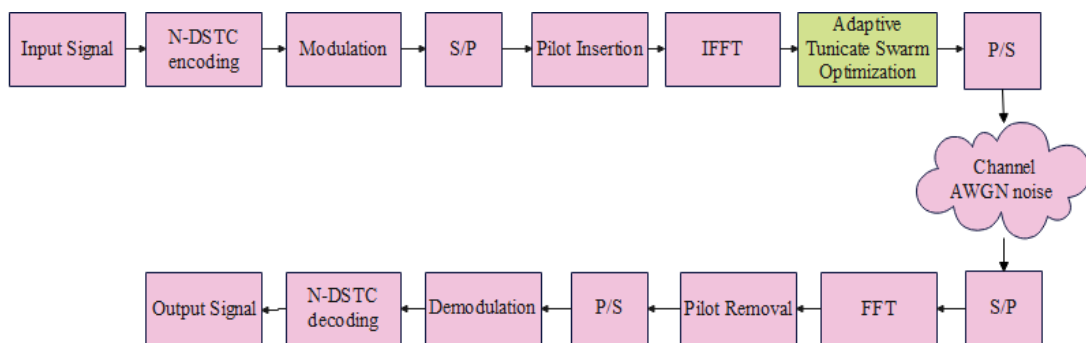


Figure 1. Workflow of the proposed method with MIMO-OFDM

At the transmitter, the incoming binary data is first grouped and mapped according to the coding scheme of N-DSTC. The QPSK symbol is the pre-specified modulation scheme utilized, and then converted into parallel signals by serial-to-parallel block. After inserting some pilots, IFFT is additionally deployed for

transmitting a sequence of data to a time-domain signal. An ATSO is inserted into the time-domain OFDM symbol to reduce the inter carrier interface (ICI) and inter symbol interference (ISI). The transmitted signal passes by using the channel with AWGN noise after the converting the signal serial into parallel. The FFT is followed after the conversion of serial to parallel at the receiver. After FFT, some pilots are removed and the system is converted from parallel to a serial block. At last, the binary data is acquired after the demodulation using the QPSK modulation scheme, and decoding using the N-DSTC coding scheme. The QPSK provides a low error probability and good noise immunity, alongside the bandwidth required by the QPSK being reduced to half as compared to binary phase-shifty keying (BPSK) for the same BER. Furthermore, IFFT is employed for transmitting the sequence of data to the time-domain signal, after inserting some pilots.

**2.1. System model of MIMO-OFDM**

In this paper, a system model of MIMO-OFDM [26], having three major portions, namely, transmitter, channel, and receiver is introduced. This approach provides an efficient and robust system for data transmission in MIMO-OFDM. Figure 2 shows the system model of MIMO-OFDM.

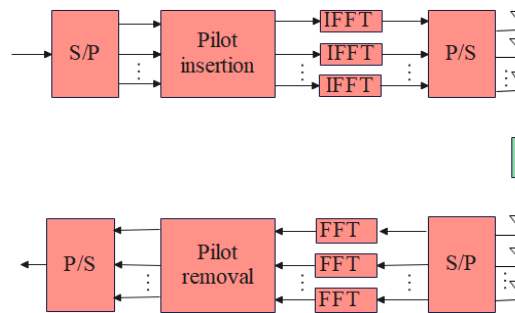


Figure 2. System model of MIMO-OFDM

The system of IFFT and FFT MIMO-OFDM is implemented in this paper. This approach provides an efficient and robust system for data transmission in MIMO-OFDM. A baseband signal is described in (1) and a time domain sample in IFFT output is expressed in (2).

$$x(t) = \sum_{k=0}^{N-1} X(k)e^{j2\pi k\Delta f t} \tag{1}$$

$$x(n) = W^H X(k) \tag{2}$$

Where,  $N$  is the number of subcarriers,  $X(k)$  is the complex modulation symbol transmitted on  $k^{th}$  subcarrier, and  $\Delta f$  is the subcarrier spacing.  $W$  is the FFT integrated matrix of order  $N \times N$ . The CP of length  $g$  is extended to remove ISI which is expressed in (3). The received signal is described in (4).

$$x'(n) = C_r \times x(n) \tag{3}$$

$$y(n) = \sum_{i=0}^{L-1} h_i x'(n - i) + z(n), n = 0, 1, \dots, N - 1 \tag{4}$$

Where,  $z(n) \sim N(0, \sigma_z^2) - AWGN$ ,  $C_r - (N + G) \times N$  is the order matrix. The frequency channels are designed by utilizing  $L$ -tap finite impulse response (FIR) using taps  $[h_0, h_1, \dots, h_{L-1}]$ . At the receiver side, the CP elimination exists that is denoted as a received signal multiplication by using a matrix  $C_R$ , and is expressed in (5) and (6).

$$C_R = [O_{N \times G} I_N] \tag{5}$$

$$Y(k) = W C_R \tilde{H} C_T W^H X(k) + Z(k) \tag{6}$$

Where,  $Z(k) = W C_R z(n)$  and  $H = W C_R \tilde{H} C_T W^H$ . Therefore, the frequency domain received signal for OFDM is provided in (7). The received signal matrix vector model is expressed in (8) and (9).

$$Y = HX + Z \tag{7}$$

$$Y = Ah + Z \quad (8)$$

$$H = \sqrt{N}Fh \quad (9)$$

Where,  $H$  is the response of channel frequency,  $X$  is the transmitted symbols,  $Z$  is the AWGN with 0 mean.  $N_t$  and  $N_r$  is the number of transmit and receive antennas in MIMO-OFDM,  $h$  is the received symbol,  $Y$  is minimum pilots.  $A = \sqrt{N}diag(X)F$  and  $F$ - partial FFT matrix and CFR matrix. The transmitted MIMO-OFDM system are provided to the N-DSTC system for the encoding and decoding processes of the OFDM signal.

## 2.2. Nonsquare matrix-based differential space-time coding

In this section, the N-DSTC consisting of encoding and decoding approaches [27], [28] are discussed. This section encodes and decodes the input of the OFDM signal, where the N-DSTC scheme is majorly utilized to minimize the number of time slots. The space-time euphemism  $S(i) \in C^{M \times M}$  is transmitted in  $M$  slots by  $M$  antennas. Enhancing a large amount of transmit antennas affects the enhancing of the number of essential time slots and ineffective for large scenarios of MIMO. Hence, a non-square matrix-based DSTC is developed to minimize the amount of time slots. Particularly, it increase  $S(i)$  through basis  $e_1 \in C^{M \times 1}$  to minimize the number of slots between  $M$  and 1.

### 2.2.1. Nonsquare differential encoding and decoding

The set of estimating metrics  $\{E_1, \dots, E_{M/T}\}$  are transmitted at the beginning of the transmission stream. Initially, the received symbol is denoted in (10). Hence, this requires  $M$  number of time slots. Considering the  $W$  blocks time transmission frame, the projection metrics are transmitted to the receiver. The subsequent data metrics  $X(i)$  are encoded and expressed in (11). Mapped onto  $M \times T$  nonsquare matrices by projection matrix  $E_i$ , as well as transmitted such that interrelated received signal is formulated in (12).

$$Y(i) = H(i)E_i + V(i), \text{ for } 1 \leq i \leq M/T \quad (10)$$

$$S(i) = \begin{cases} I_M \text{ if } i = \frac{M}{T}, \text{ or} \\ S(i-1)X(i) \text{ if } i > \frac{M}{T}, \end{cases} \quad (11)$$

$$Y(i) = H(i)S(i)E_i + V(i), \text{ for } \frac{M}{T} < i \leq W \quad (12)$$

The ratio among the number of transmit antennas  $M$  and length of frame  $W$  is,  $\eta \triangleq M/W$  which is denoted as an insertion ratio. For the task performance, this method sets  $\eta = 5\%$  such that  $W = 200M$ , but remark that the N-DSTC performance remains robust in high-speed mobile scenarios plan using  $\eta = 1\%$  or  $0.1\%$ . Hence, the tree-based approach is utilized to achieve minimum PAPR between all sub-carriers in a limited computational process. In the process of phase factor, the proposed algorithm accumulates the phase factor yielding less PAPR. To achieve this, the proposed method uses the ATSO model for obtaining reduced PAPR values. The obtained results are provided to the optimization algorithm for the further processes.

## 3. TUNICATE SWARM OPTIMIZATION

The encoded data from the input signal is provided to the optimization process for improving the computational efficiency of the phase optimization algorithm. Tunicate swarm optimization (TSO) [29] is a meta-heuristic algorithm activated by marine tunicates' performance and jet propulsion over navigation as well as foraging. The tunicate is in the form of a millimeter scale and locates sources of food in the sea. The tunicate satisfies the three general conditions in propulsion which are: to eliminate the hit using the number of tunicates in search space, to obtain a suitable path to select an effective search location, and finally, to select a better search agent. Further, the tunicates change their positions to achieve better search, and the process is enhanced in every iteration. The TSO begins using population incidentally produces tunicate with generate variables permissible boundaries, as expressed in (13) where tunicates modify the location in iterations as depicted in (14).

$$\vec{T}_p = \vec{T}_p^{min} + rand \times (\vec{T}_p^{max} - \vec{T}_p^{min}) \quad (13)$$

$$\vec{T}_p(\vec{x} + 1) = \frac{\vec{T}_p(x) + \vec{T}_p(\vec{x})}{2 + c_1} \tag{14}$$

Where,  $\vec{T}_p$  is the tunicate position,  $rand$ ,  $c_1$  denotes arbitrary number within the range [0,1].  $\vec{T}_p^{max}$  and  $\vec{T}_p^{min}$  are the lower and upper design variables, respectively, while  $\vec{T}_p(x)$  is the updated position of tunicate’s food source as mathematically expressed in (15).  $SF$  is the source of food,  $A$  is the arbitrary vector that avoids the tunicates from hitting one another and it is mathematically designed in (16).

$$\vec{T}_p(x) = \begin{cases} SF + A \times |SF - rand \times \vec{T}_p|, & \text{if } rand \geq 0.5 \\ SF - A \times |SF - rand \times \vec{T}_p| & \text{if } rand < 0.5 \end{cases} \tag{15}$$

$$A = \frac{c_2 + c_3 - 2c_1}{VT_{min} + c_1(VT_{max} - VT_{min})} \tag{16}$$

Where,  $c_1$ ,  $c_2$  and  $c_3$  – random number with range [0,1],  $VT_{min}$ , while  $VT_{max}$  respectively reflect minimum and maximum speeds utilized to perform community communication denoted as 0 and 1. The obtained TSO outcome is provided in the next section for the efficient reduction of PAPR. The TSO algorithm procedures are given:

- Initialize the population of tunicate  $\vec{T}_p$  according to (13).
- Select initial parameters as well as a greater number of iterations.
- Estimate the fitness value of the search agent.
- The better tunicate is traversed in given search space.
- Update the tunicate’s position utilizing (14).
- Alter the updated tunicate that moves behind a boundary in the provided search space.
- Calculate the updated fitness value of the tunicate. If it obtains the best solution than the preceding optimal solution, it is updated with a better solution.
- If satisfied with an ending basis, then the algorithm ends or repeats steps 5 to 8.
- Finally, the best solution has been obtained.

**3.1. Adaptive tunicate swarm optimization**

The efficiency of the tunicate swarm algorithm (TSA) exhibits endurance with the local optimum solutions when compared to the most common algorithms. Moreover, this is not better choice for certain intricate solutions by various optimal solutions. In TSA, each tunicate finds the food source and finds it unfeasible to retrieve without knowing where the food source is located. Later, it achieves convergence when it is no longer able to design findings and ends functioning. Thus, an adaptive version of TSO (ATSO) [30] is implemented to defeat weaknesses in TSO as well as improve the algorithm’s search capacity and flexibility. The TSO is improved by using the two phases such as exploration and exploitation to enhance the search capability. Figure 3 shows the proposed method using ATSO.

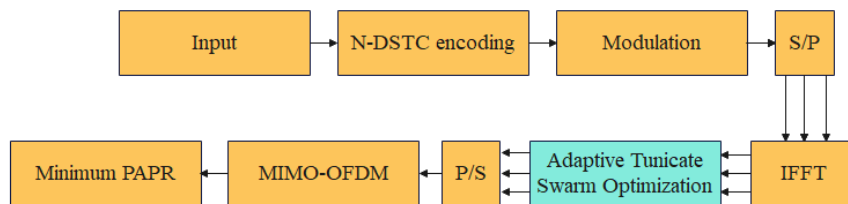


Figure 3. The proposed method using ATSO

An efficient metaheuristic algorithm is essential to classify the process of search into multiple phases of exploration and exploitation. The metaheuristic algorithm is employed to find a good solution to an optimization problem that is complex and difficult to solve to optimality. Conversely, the exploitation denotes the optimization algorithm’s capacity to identify near-optimal solutions. The exploitation permits the optimizer to focus on closets that compromise good quality solutions in the space of searching. As each iteration passes, TSO updates the candidate position solutions near individual points to the entire population in such a way that the TSO has a good capability of exploitation. Thus, its drawback is the absence of efficient global search, alongside rejecting an exploration capability.

Aiming to enhance the algorithm's establishment and exploration capacity, the introduced ATSO carries out two major phases in every iteration. Initially, the candidate solution is selected incidentally in place of a better solution, and the location of the applicant solutions is updated based on arbitrary tunicate's location. The optimizer employs an arbitrary operator to analyze diverse areas and search space for efficient exploration. Hence, in ATSO, two different incident numbers are calculated in a tunicate updating eqn. to generate solutions in different search space areas. An ATSO exploration phase is logically expressed in (17).

$$\vec{T}_p(\vec{x} + 1) = \vec{T}_p(r) - rand_1 \times |\vec{T}_p(r) - 2 \times rand_2 \times \vec{T}_p(\vec{x})| \quad (17)$$

Where,  $\vec{T}_p(r)$  arbitrarily chosen tunicate that forms a new population. This process encourages exploration, as well as permits the TSO to perform many robust global searches using the entire space of search. In the last phase, the tunicate updates its positions according to the best tunicate position. Moreover, in the ATSO, the lowest tunicate using the greatest aiming function value is changed using an incidentally produced tunicate at every iteration. The exploration and exploitation of ATSO in search space are controlled by the inertia constant instead of using the mathematical equation. The ATSO algorithm eminently enhances the computational efficiency of the phase optimization algorithm.

Eventually, the optimal phase factors are acquired by an optimization algorithm, and further, this algorithm provides the maximal optimal phase factors by the utilization of ATSO. However, the optimization algorithm consumes a minimum duration than the other methods and hence, the computational time is decreased by utilizing the ATSO algorithm. Further, the evaluation and implementation of this proposal is provided in the following sections.

#### 4. RESULTS AND DISCUSSION

In this research, an ATSO-PTS method is proposed to reduce PAPR values in a waveform of OFDM signal. The proposed method is implemented on the MATLAB software, on a system operated with an i5 processor and 6 GB RAM. The proposed ATSO-PTS method is utilized to perform an effective denoising and channel estimation for MIMO-OFDM. The performance of the proposed ATSO-PTS method is compared with the existing methods. The existing methods namely, OFDM, conventional-PTS (C-PTS), conventional-selective mapping (C-SLM), and PSO are utilized for the comparison. Furthermore, the performance metrics used in this research to evaluate the performance of the proposed ATSO-PTS are, BER, PAPR, complementary cumulative distribution function (CCDF), and symbol error rate (SER). The parameter settings of this model are depicted in Table 1.

Table 1. Parameter settings of the ATSO-PTS method

Parameter	Value
Number of iterations	100
Population size	30
User carriers	52, 104, 156, 208, 260
Pilot carriers	12, 24, 48, 60, 72
FFT size	64, 128, 256, 512, 1024
Antenna	$2 \times 2$ , $2 \times 4$ , $4 \times 2$ , $4 \times 4$
Number subcarriers	128, 256
Cyclic prefix or guard time	0 to 2e-6s
Modulation	QPSK
Modulation range	16
MIMO-OFDM symbols	16
Oversampling factor	1e6 HZ
Channel type	AWGN channel

Table 2 represents the  $E_b/N_o$ (dB) comparison for the proposed method against the existing methods when the value is taken as 30. The existing methods of OFDM, BPSK, QAM-8 and QAM-16 are measured and compared with the proposed method. Figure 4 shows the graphical representation of BER, with respect to  $E_b/N_o$ (dB).

In Table 2, the QPSK modulation is compared with previous modulations using BER. The maximum BER with respect to  $E_b/N_o$ (dB) of QPSK modulation is 30 dB. The maximum BER with respect to BER of the QPSK of value is 30 dB. The PAPR reduction is achieved without downgrading the performance of BER, in contrast to the existing methods. Here, the AWGN noise channel is considered



where the  $E_b/N_o(dB)$  ranges between -30 to 30. The BER values and error number are minimized because of its enhanced noise immunity and low error probability.

Table 2. Performance analysis of BER in  $E_b/N_o(dB) = 30$

Methods	BER
OFDM	$10^{-3.4}$
BPSK	$10^{-3.8}$
QAM-8	$10^{-3.4}$
QAM-16	$10^{-1.5}$
QPSK	$10^{-7.4}$

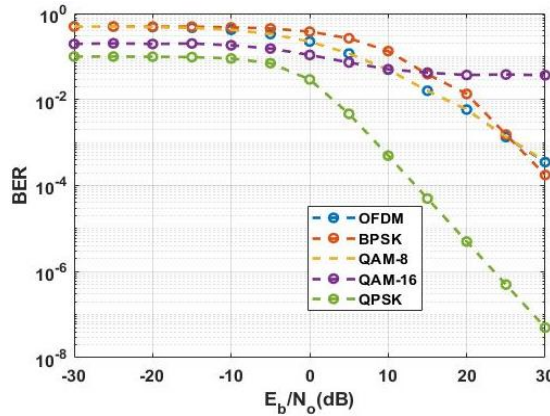


Figure 4. Graphical representation of BER of the QPSK modulation in MIMO-OFDM

Table 3 represents the  $E_b/N_o(dB)$  comparison of the proposed method with that of the competitor approaches when the value is 30. The existing methods, which are OFDM, C-PTS, C-SLM, and PSO are measured and compared with the proposed method. Figure 5 represents the graphical representation of BER as to  $E_b/N_o(dB)$ .

Table 3. Performance comparison of BER when  $E_b/N_o(dB) = 30$

Methods	BER
OFDM	$10^{-4.8}$
C-PTS	$10^{-5}$
C-SLM	$10^{-5.8}$
PSO	$10^{-6.5}$
Proposed ATSO	$10^{-8.2}$

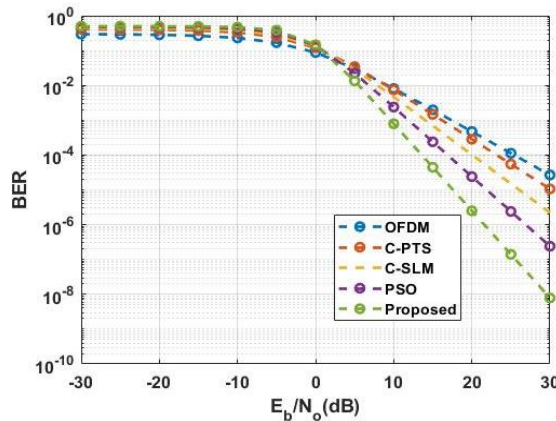


Figure 5. Graphical representation of BER of proposed ATSO-PTS method in MIMO-OFDM with respect to  $E_b/N_o(dB)$



In Table 3, the proposed ATSO-PTS is compared with the existing modulations in terms of BER. The BER with  $E_b/N_o(dB)$  of the ATSO-PTS value is set to 30 dB. Here, without downgrading the performance of BER, the PAPR reduction is achieved contrasting to other methods. Here, the AWGN noise channel is considered where the  $E_b/N_o(dB)$  is in the range of -30 to 30. The values of the BER are reduced because of its enhanced noise immunity and low error probability.

Table 4 represents the PAPR (dB) comparison of the proposed method QPSK with competitor approaches when  $CCDF = 10^{-2.5}$ . The QPSK is compared with existing modulations, OFDM, BPSK, QAM-8, and QAM-16. Figure 6 shows the graphical illustration of CCDF with respect to PAPR (dB).

Table 4. Performance comparison of QPSK using PAPR (dB) when  $CCDF=10^{-2.5}$

Methods	PAPR (dB)
OFDM	18.3
BPSK	7.5
QAM-8	9.1
QAM-16	7
QPSK	2.5

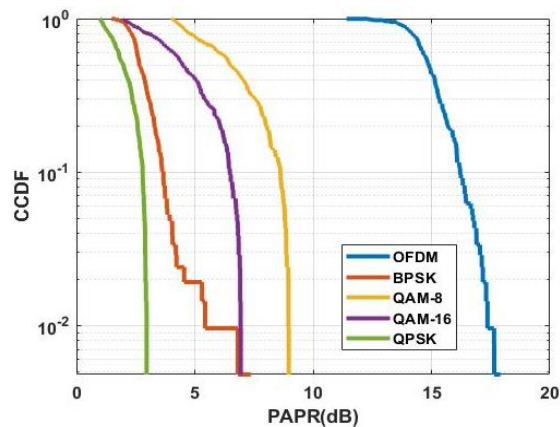


Figure 6. Graphical representation of QPSK modulation and various existing methods based on CCDF

In Table 4, the QPSK is compared with existing modulations in terms of CCDF with PAPR (dB). A maximum CCDF using PAPR of QPSK is 2.5 dB. The OFDM achieves 18.3 dB, BPSK achieves 7.5 dB, QAM-8 achieves 9.1 dB, and QAM-16 achieves 7 dB. The suggested ATSO-PTS method achieves the PAPR values multiple times better than the original OFDM. The PAPR range lies between 0 and 20.

Table 5 represents the PAPR (dB) comparison of the proposed method ATSO with existing methods when  $CCDF = 10^{-2.5}$ . The proposed ATSO-PTS is compared with previous modulations, OFDM, C-PTS, C-SLM, and PSO. Figure 7 shows the graphical illustration of CCDF in terms of PAPR (dB).

Table 5. Performance analysis of ATSO using PAPR (dB) in  $CCDF = 10^{-2.5}$

Methods	PAPR (dB)
OFDM	18.5
C-PTS	9.8
C-SLM	8.5
PSO	6.5
Proposed ATSO	2.9

In Table 5, the suggested ATSO-PTS is compared with previous modulations in terms of PAPR (dB). A CCDF in terms of PAPR of ATSO-PTS is 2.9 dB. The OFDM achieves 18.5 dB, C-PTS achieves 9.8 dB, C-SLM achieves 8.5 dB, and PSO achieves 6.5 dB. The proposed ATSO-PTS method achieves the PAPR values multiple times better than the original OFDM. The PAPR range lies between 0 and 20.

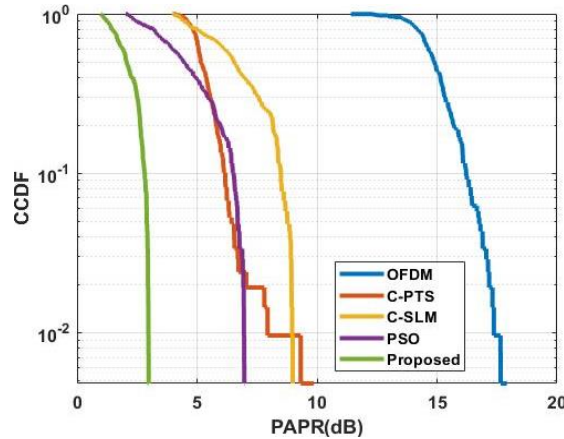


Figure 7. Graphical representation of proposed ATSO-PTS and various existing methods

Table 6 represents the  $E_b/N_o$  (dB) comparison of the proposed method with competitor approaches at a value of 30. The QPSK modulation is compared with existing modulations named OFDM, BPSK, QAM-8, and QAM-16. Figure 8 shows the graph of SER with respect to  $E_b/N_o$  (dB).

In Table 6 the QPSK modulation is compared with previous modulations in terms of SER. The maximum SER with respect to  $E_b/N_o$  (dB) of QPSK modulation is 30 dB. The maximum BER in terms of BER of the QPSK of value is 30 dB. Without downgrading the performance of BER, the PAPR reduction is achieved compared to other methods. Here, the AWGN noise channel is considered, and the  $E_b/N_o$  (dB) in the range between -30 to 30. The SER values are reduced because of its enhanced noise immunity and low error probability.

Table 6. Performance comparison of SER when  $E_b/N_o$  (dB)=30

Methods	SER
OFDM	$10^{-5.7}$
BPSK	$10^{-6.7}$
QAM-18	$10^{-3.7}$
QAM-16	$10^{-3.8}$
QPSK	$10^{-8.5}$

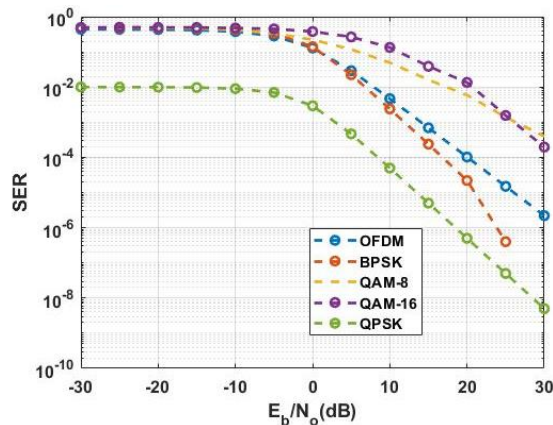


Figure 8. Graphical representation of SER of the QPSK modulation in MIMO-OFDM

Table 7 represents the  $E_b/N_o$  (dB) comparison of the proposed method with competitor approaches at a value is 30. The proposed ATSO-PTS is compared with the existing modulations like OFDM, C-PTS, C-SLM, PSO. Figure 9 shows the graphical representation of SER with respect to  $E_b/N_o$  (dB).

In Table 7, the proposed ATSO-PTS is compared with the existing modulations as to SER. The  $E_b/N_o$  (dB) of the proposed ATSO-PTS achieved the maximum SER value is 30 dB. Without downgrading

the performance of SER, the PAPR reduction is achieved compared to other methods. The values of the SER are reduced because of its enhanced noise immunity and low error probability.

Table 7. Performance analysis of SER in  $E_b/N_o$  (dB)=30

Methods	SER
OFDM	$10^{-4.5}$
C-PTS	$10^{-5}$
C-SLM	$10^{-5.8}$
PSO	$10^{-6.8}$
Proposed ATSO-PTS	$10^{-8.2}$

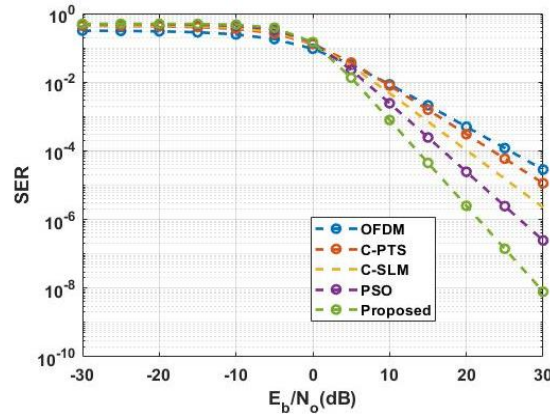


Figure 9. Graphical representation of SER of proposed ATSO-PTS method in MIMO-OFDM

#### 4.1. Comparative analysis

This section demonstrates the comparative analysis of ATSO-PTS with the BER and PAPR as shown in Table 8. Table 9 represents the comparative analysis of ATSO-PTS with the 10 dB of BER and SNR. Existing research such as [16]–[18] are used for evaluating the ability of the proposed method. The proposed ATSO-PTS achieved a 2.9 PAPR compared to the TSHO-PTS method.

Table 8. Comparative analysis of proposed method with existing methods with 30 PAPR

Author	Method	PAPR (dB)
Sarkar <i>et al.</i> [16]	TSHO-PTS	5
Sidiq <i>et al.</i> [17]	ABC-SLM-PTS	5.6
Kumar <i>et al.</i> [18]	PSO-GWO	10.1
Proposed ATSO-PTS	ATSO-PTS	2.9

Table 9. Comparative analysis of the proposed method with existing methods using 30 dB with BER and SER

Author	Method	BER	SNR
Sarkar <i>et al.</i> [16]	TSHO-PTS	0.01	0.01
Sidiq <i>et al.</i> [17]	SLM-PTS	0.07	0.12
Kumar <i>et al.</i> [18]	PS-GW-PTS	0.03	0.02
Proposed ATSO-PTS	ATSO-PTS	0.01	0.025

#### 4.2. Discussion

This section discusses the obtained results of the proposed method compared with the existing methods. The OFDM approach's values of the PAPR are reduced by the outcomes of existing methods as well as ATSO performance in PTS. In this proposed method, the number of parameters is carried out to reduce the PAPR rate in OFDM signals. The various simulations are carried out to identify a PAPR improvement for the determination and comparison of the sub-optimal PTS. A single OFDM is produced arbitrarily to minimize the PAPR as well and corresponding parameters are performed for the process of simulation. The obtained classification results of this research are represented in Tables 1 to 6. Figures 4 to 9 shows the graphical representation of the reduction of BER, PAPR, and SER. Table 8 shows the comparative analysis of the proposed method with existing methods with 30 PAPR. In Table 8 the existing methods such as TSHO-PTS [16] have achieved a PAPR (dB) rate of 5. The ABC-SLM-PTS [17] have achieved a PAPR rate of 5.6, PSO-GWO [18] achieved the 10.1 PAPR (dB). The proposed ATSO-PTS method has achieved a better result with PAPR value is 2.9 respectively. Table 9 shows the BER and SNR reduction of the proposed method with existing methods. In Table 9, the existing method of TSHO-PTS [16] has achieved the 0.01

BER and SNR rate for 30 dB PAPR. The ABC-SLM-PTS [17] have achieved the BER rate 0.07 and SNR of 0.12. The PSO-GWO [18] achieved a BER of 0.03 and SNR of 0.02. The proposed ATSO-PTS method has achieved better results on BER is 0.01 and 0.025 respectively. The proposed method achieves a fast convergence speed compared with the other methods.

## 5. CONCLUSION

MIMO and OFDM are majorly utilized in wireless systems and wired high-data rate communications. In this research, the ATSO-PTS algorithm is proposed for the PAPR reduction in the MIMO-OFDM signal. The phase optimization is taken out in the OFDM signal with PTS and the proposed method is tested with FFT in OFDM signal optimization. The proposed method achieved better PAPR reduction when compared to the existing research methods by utilizing the optimization ATSO technique. In the MIMO-OFDM signal, the ATSO optimization algorithm is applied to reduce the PAPR as well as reduce the computational complexity of the phase optimization. The ATSO-PTS achieved less PAPR, BER, and SNR compared to other methods. The proposed method has 10-2 CCDF in 2.9 PAPR as well as existing TSHO-PTS method obtained the 5.0 PAPR to achieve 10-2 CCDF. The future work of the proposed method involves combining multiple PAPR reduction techniques into a hybrid scheme which can potentially lead to better performance.





## REFERENCES

- [1] D. V. Linh and V. V. Yem, "Key generation technique based on channel characteristics for MIMO-OFDM wireless communication systems," *IEEE Access*, vol. 11, pp. 7309–7319, 2023, doi: 10.1109/ACCESS.2023.3238573.
- [2] Z. Gao *et al.*, "Data-driven deep learning based hybrid beamforming for aerial massive MIMO-OFDM systems with implicit CSI," *IEEE Journal on Selected Areas in Communications*, vol. 40, no. 10, pp. 2894–2913, Oct. 2022, doi: 10.1109/JSAC.2022.3196064.
- [3] A. Arvola, S. K. Joshi, A. Tolli, and D. Gesbert, "PAPR reduction in MIMO-OFDM via power efficient transmit waveform shaping," *IEEE Access*, vol. 10, pp. 47906–47920, 2022, doi: 10.1109/ACCESS.2022.3172325.
- [4] S. N. Rani and G. Indumathi, "Chicken swarm optimization based optimal channel allocation in massive MIMO," *Wireless Personal Communications*, vol. 129, no. 3, pp. 2055–2077, Apr. 2023, doi: 10.1007/s11277-023-10225-6.
- [5] X.-F. Kang, Z.-H. Liu, and M. Yao, "Deep learning for joint pilot design and channel estimation in MIMO-OFDM systems," *Sensors*, vol. 22, no. 11, p. 4188, May 2022, doi: 10.3390/s22114188.
- [6] Z. Liu *et al.*, "Low-complexity PAPR reduction method for OFDM systems based on real-valued neural networks," *IEEE Wireless Communications Letters*, vol. 9, no. 11, pp. 1840–1844, Nov. 2020, doi: 10.1109/LWC.2020.3005656.
- [7] V. Padarti and V. Nandhanavanam, "An improved ASOICF algorithm for PAPR reduction in OFDM systems," *International Journal of Intelligent Engineering and Systems*, vol. 14, no. 2, pp. 353–360, Apr. 2021, doi: 10.22266/ijies2021.0430.32.
- [8] Y. Cao, T. Lv, and W. Ni, "Two-timescale optimization for intelligent reflecting surface-assisted MIMO transmission in fast-changing channels," *IEEE Transactions on Wireless Communications*, vol. 21, no. 12, pp. 10424–10437, Dec. 2022, doi: 10.1109/TWC.2022.3184000.
- [9] V. G. Tikka and R. Sivashanmugam, "Error correction using hybrid coding algorithm for BER reduction in MIMO-OFDM," *International Journal of Intelligent Engineering and Systems*, vol. 15, no. 6, pp. 618–626, Dec. 2022, doi: 10.22266/ijies2022.1231.55.
- [10] D. K. Onebunne, C. A. Nwabueze, B. O. Ekengwu, and P. C. Odukwue, "Improving bit error rate of MIMO-OFDM system using discrete wavelet transformation," *International Journal of Advanced Networking and Applications*, vol. 14, no. 2, pp. 5378–5384, 2022.
- [11] S. Jothi and A. Chandrasekar, "An efficient modified dragonfly optimization based MIMO-OFDM for enhancing qos in wireless multimedia communication," *Wireless Personal Communications*, vol. 122, no. 2, pp. 1043–1065, Jan. 2022, doi: 10.1007/s11277-021-08938-7.
- [12] C. Sun, J. Zhao, J. Wang, L. Xia, X. Gao, and Q. Wang, "Beam domain MIMO-OFDM optical wireless communications with PAPR reduction," *IEEE Photonics Journal*, vol. 15, no. 2, pp. 1–10, Apr. 2023, doi: 10.1109/JPHOT.2023.3246487.
- [13] E. F. Badran, M. Samara, and N. E. Ismail, "Carrier frequency offset estimation for MIMO single-carrier FDMA system in wireless communication," *Alexandria Engineering Journal*, vol. 61, no. 9, pp. 6907–6917, Sep. 2022, doi: 10.1016/j.aej.2021.12.036.
- [14] S. S. P. Kumar, C. A. Kumar, and R. J. Rose, "An efficient SLM technique based on chaotic biogeography-based optimization algorithm for PAPR reduction in GFDM waveform," *Automatika*, vol. 64, no. 1, pp. 93–103, Jan. 2023, doi: 10.1080/00051144.2022.2106532.
- [15] Z. Duan and F. Zhao, "Pilot allocation and data power optimization based on access point selection in cell-free massive MIMO," *Wireless Communications and Mobile Computing*, vol. 2022, pp. 1–10, Apr. 2022, doi: 10.1155/2022/4044783.
- [16] M. Sarkar, A. Kumar, and B. Maji, "PAPR reduction using twin symbol hybrid optimization-based PTS and multi-chaotic-DFT sequence-based encryption in CP-OFDM system," *Photonic Network Communications*, vol. 41, no. 2, pp. 148–162, Apr. 2021, doi: 10.1007/s11107-020-00923-7.
- [17] S. Sidiq, J. A. Sheikh, F. Mustafa, B. A. Malik, and I. B. Sofi, "PAPR minimization of FBMC/OQAM scheme by hybrid SLM and PTS using artificial: bee-colony phase—optimization," *Arabian Journal for Science and Engineering*, vol. 46, no. 10, pp. 9925–9934, Oct. 2021, doi: 10.1007/s13369-021-05625-4.
- [18] P. R. Kumar, P. V. Naganjaneyulu, and K. S. Prasad, "Hybrid PS–GW optimised PTS scheme for PAPR reduction in OFDM system," *IET Communications*, vol. 13, no. 18, pp. 2996–3002, Nov. 2019, doi: 10.1049/iet-com.2019.0261.
- [19] S. Prasad and R. Jayabalan, "PAPR reduction in OFDM using scaled particle swarm optimisation based partial transmit sequence technique," *The Journal of Engineering*, vol. 2019, no. 5, pp. 3460–3468, May 2019, doi: 10.1049/joe.2018.5340.
- [20] Ş. Şimşir and N. Taşpınar, "A novel discrete elephant herding optimization-based PTS scheme to reduce the PAPR of universal filtered multicarrier signal," *Engineering Science and Technology, an International Journal*, vol. 24, no. 6, pp. 1428–1441, Dec. 2021, doi: 10.1016/j.jestch.2021.03.001.





- [21] J. Bai and S. Yang, "In UOWC systems: a combined PAPR reduction method by PTS approach based on improved particle swarm optimization," *Optik*, vol. 232, p. 166581, Apr. 2021, doi: 10.1016/j.ijleo.2021.166581.
- [22] A. K. Abed, R. Mansoor, and A. K. Abed, "Particle swarm optimization-based dummy sub-carriers insertion for peak to average power ratio reduction in OFDM systems," *JCT Express*, vol. 8, no. 1, pp. 135–141, Mar. 2022, doi: 10.1016/j.jcte.2021.07.005.
- [23] L. Li, L. Xue, X. Chen, and D. Yuan, "Partial transmit sequence based on discrete particle swarm optimization with threshold about PAPR reduction in FBMC/OQAM system," *IET Communications*, vol. 16, no. 2, pp. 142–150, Jan. 2022, doi: 10.1049/cmu2.12321.
- [24] Ş. Şimşir and N. Taşpınar, "An improved PTS scheme based on a novel discrete invasive weed optimization algorithm for PAPR reduction in the UPMC signal," *Neural Computing and Applications*, vol. 33, no. 23, pp. 16403–16424, Dec. 2021, doi: 10.1007/s00521-021-06237-7.
- [25] T. H. Ali and A. Hamza, "Low-complexity PAPR reduction method based on the TLBO algorithm for an OFDM signal," *Annals of Telecommunications*, vol. 76, no. 1–2, pp. 19–26, Feb. 2021, doi: 10.1007/s12243-020-00777-0.
- [26] I. Khan, M. Cheffena, and M. M. Hasan, "Data aided channel estimation for MIMO-OFDM wireless systems using reliable carriers," *IEEE Access*, vol. 11, pp. 47836–47847, 2023, doi: 10.1109/ACCESS.2023.3269659.
- [27] Y. Katsuki, G. T. F. de Abreu, K. Ishibashi, and N. Ishikawa, "Noncoherent massive MIMO with embedded one-way function physical layer security," *IEEE Transactions on Information Forensics and Security*, vol. 18, pp. 3158–3170, 2023, doi: 10.1109/TIFS.2023.3277255.
- [28] Y. Katsuki and N. Ishikawa, "Optimal but low-complexity optimization method for nonsquare differential massive MIMO," in *2021 IEEE 94th Vehicular Technology Conference (VTC2021-Fall)*, IEEE, Sep. 2021, pp. 1–5. doi: 10.1109/VTC2021-Fall52928.2021.9625337.
- [29] D. A. Disney and A. Merline, "An improved fuzzy logic-based small cell deployment in NOMA-HetNet: a novel sun flower-based tunicate swarm optimization-oriented multi objective concept," *Sādhanā*, vol. 48, no. 2, p. 67, Apr. 2023, doi: 10.1007/s12046-023-02123-1.
- [30] A. Arabali, M. Khajehzadeh, S. Keawsawasvong, A. H. Mohammed, and B. Khan, "An adaptive tunicate swarm algorithm for optimization of shallow foundation," *IEEE Access*, vol. 10, pp. 39204–39219, 2022, doi: 10.1109/ACCESS.2022.3164734.

## BIOGRAPHIES OF AUTHORS







**Abdul Lateef Haroon Phulara Shaik**     received a B.E. in electronics and communication engineering RYMEC, Ballari, Karnataka, India. He holds an M.Tech. degree in VLSI design and embedded systems from K S School of Engineering and Management, Karnataka, India. Obtained a Ph.D. in electrical engineering sciences from Visvesvaraya Technological University Belagavi, Karnataka, India. Currently, he is an associate professor in the Department of Electronics and Communication Engineering at BITM Ballari, Karnataka, India. He has published many papers in International and National journals and international conference proceedings and has three patents. At present, he is guiding four students at Visvesvaraya Technological University, Belagavi, and Karnataka, India. He has around 12 years of teaching and research experience. He can be contacted at email: [abdul.lh@bitm.edu.in](mailto:abdul.lh@bitm.edu.in).






**Sowmya Madhavan**     is presently working as an associate professor in the Department of Electronics and Communication Engineering, Nitte Meenakshi Institute of Technology, Bangalore. She completed her bachelor of engineering in telecommunication and master of technology in Digital Electronics from Visvesvaraya Technological University, Belgaum. She has also completed her Ph.D. from Visvesvaraya Technological University, Belgaum. She has published about 18 papers in various journals and conferences. She has also completed her PG level advanced certification program in VLSI chip design. Her research interests are physical design, RTL design and analog VLSI design. She can be contacted at email: [sowmya.madhavan@nmit.ac.in](mailto:sowmya.madhavan@nmit.ac.in).






**Parameshchhari Bidare Divakarachari**     currently working as a professor in the Department of Electronics and communication Engineering at Nitte Meenakshi Institute of Technology, Bengaluru, Karnataka, India affiliated to Visvesvaraya Technological University (VTU), Belagavi, Karnataka, India. He is also the visiting professor for University of Rome Tor Vergata, Italy. He is currently serving as the student activity committee chair, IEEE Bangalore Section. He is also listed in the World's Top 2% Scientist by Stanford University, USA for his research works. He has published over 150+ articles in SCI, Scopus and other indexed journals and in several international conferences. He is the associate editor for Expert Systems (Wiley), International Journal of Computational Intelligence Systems (Springer), Wireless Communication and Mobile Computing (Hindawi) and International Journal of Reconfigurable and Embedded Systems (IAES). He is also serving as editorial board member, academic editor and reviewer for several international journals indexed in SCI and Scopus. He has also served as the lead guest editor for Springer, Elsevier and IEEE Journals. Under his guidance, IEEE NMIT SB has received Rs. 20,000,000 funding from IEEE AESS Society. He can be contacted at email: [paramesh@nmit.ac.in](mailto:paramesh@nmit.ac.in).








**Rocío Pérez de Prado**    received the M.S. degree in telecommunication engineering from University of Seville, Spain, in 2008, and the Ph.D. degree in Telecommunication Engineering with European Mention from University of Jaén, Spain, in 2011. At present, she is an associate professor at the Department of Telecommunication Engineering at the University of Jaén, Spain, with more than 15 years of research experience in the fields of artificial intelligence, machine learning, data science, cloud-IoT-edge, and telecommunications. In 2021, she was appointed as IEEE Senior Member. She has authored more than 60 research publications (35 in journals indexed in JCR). Since 2021 she works as an expert for the European Commission evaluating projects for H2020 and Marie Skłodowska-Curie Actions, and since 2020 she has been an external evaluator and member of project selection committees of the National Fund for Scientific and Technological Development, for the government of Peru. She is an associate editor of the official journal of the World Federation of Soft-Computing, Applied Soft Computing, Elsevier, editor in engineering applications of artificial intelligence, Elsevier, editor in Intelligent Automation and Soft-Computing, Tech Science Press, and Energies, MDPI, and has edited more than 10 special issues in diverse JCR-indexed journals and 2 international books. She has also served as reviewer for more than 40 JCR-indexed journals. Additionally, she has participated in scientific committees/organizing committees in more than 50 international conferences such as IEEE-FUZZ between the years 2019-2023, as well as technical committee chair and track chair and keynote speaker-guest of honour at diverse conferences. Likewise, she has participated in 10 research projects and diverse contracts with companies and projects to promote entrepreneurial culture in the field of telecommunications engineering. She has received 3 awards from Publons-Clarivate Analytics, as an outstanding reviewer. In 2010 she enjoyed a 5-month stay at the Technical University of Dortmund as a visiting researcher in the Department of Systems and Control Engineering, Germany. In the teaching field, she currently teaches in 2 degrees and 3 master's degrees in the field of telecommunication engineering, artificial intelligence and cloud computing in the University of Jaén. In addition, she has supervised more than 25 bachelor's degree, master's degree and final year theses. She is the author of more than 15 teaching publications in conferences, 3 books, and she has participated in 8 teaching innovation projects (leading 2 of them). She has received 2 awards from the University of Jaén, Spain, for Good Teaching Practices Perceived by Students. She can be contacted at email: rperez@ujaen.es.



**Paramesh Siddappa Parameshwarappa**    is currently working as an assistant professor in the Department of Computer Science and Engineering, School of Engineering, Central University of Karnataka, Kalburagi, India. He received M.E. in web technology from U.V.C.E, Bangalore University in 2014 and Ph.D. in computer science and engineering from Visvesvaraya Technological University (VTU), Belagavi, India in 2022. His research areas include data mining, artificial intelligence, pattern recognition, machine learning, NLP, and soft computing techniques. He can be contacted at email: parameshsp@cuk.ac.in.



**Kavitha Malali Vishveshwarappa Gowda**    is currently working as an associate professor in Department of Electronics and Communication Engineering at Gopalan College of Engineering and Management, Karnataka, India which is affiliated to Visvesvaraya Technological University (VTU). She received M.Tech. in VLSI design and embedded system from VTU in 2009. Her Ph.D. is in VLSI design from VTU and awarded in 2021. Her research area includes VLSI design and communication. She can be contacted at email: kavishanthagiri@gmail.com.